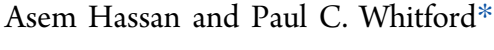


pubs.acs.org/JPCB Article

Identifying Strategies to Experimentally Probe Multidimensional Dynamics in the Ribosome

Published as part of The Journal of Physical Chemistry virtual special issue "Jose Onuchic Festschrift".





Cite This: J. Phys. Chem. B 2022, 126, 8460-8471



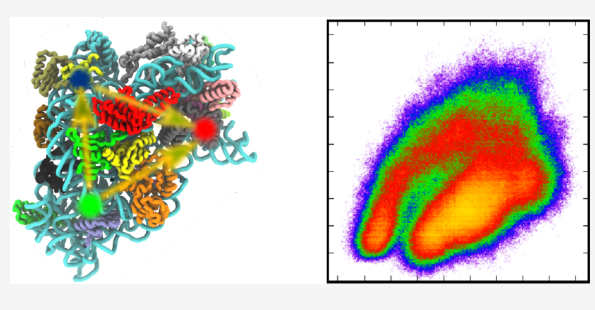
ACCESS

III Metrics & More

Article Recommendations

SI Supporting Information

ABSTRACT: The ribosome is a complex biomolecular machine that utilizes large-scale conformational rearrangements to synthesize proteins. For example, during the elongation cycle, the "head" domain of the ribosomal small subunit (SSU) is known to undergo transient rotation events that allow for movement of tRNA molecules (i.e., translocation). While the head may exhibit rigid-body-like properties, the precise relationship between experimentally accessible probes and multidimensional rotations has yet to be established. To address this gap, we perform molecular dynamics simulations of the translocation step of the elongation cycle in the ribosome, where the SSU head spontaneously



undergoes rotation and tilt-like motions. With this data set (1250 simulated events), we used statistical and information-theory-based measures to identify possible single-molecule probes that can isolate SSU head rotation and head tilting. This analysis provides a molecular interpretation for previous single-molecule measurements, while establishing a framework for the design of next-generation experiments that may precisely probe the mechanistic and kinetic aspects of the ribosome.

INTRODUCTION

Cells harbor many intricate molecular machines that perform a myriad of functions. Some notable examples include the spliceosome, proteasome, fatty acid synthetase, and nuclear pore complex. Probably the most well studied assembly is the ribosome (Figure 1a), for which more than 1500 structures have been resolved through X-ray crystallography^{1–4} and cryoelectron microscopy^{5–7} (see ref 8 for complete list). In addition, biochemical^{9–12} and single-molecule^{13–21} methods have been applied extensively to characterize the dynamics of the ribosome. With the availability of this vast body of experimental data, one may consider the ribosome an ideal system for developing a physicochemical understanding of the principles that control large-scale conformational transitions in biomolecular assemblies.

The ribosome is a massive (>2MDa, ≈ 25 nm in dimensions) ribonucleoprotein machine that is used by all living cells to synthesize proteins. All ribosomes consist of a large subunit (LSU) and a small subunit (SSU; Figure 1a). In bacteria, the LSU is composed of two rRNA (rRNA) chains (23S and 5S) and more than 30 proteins. The SSU, which is roughly 1MDa in scale, contains the 16S rRNA and approximately 20 proteins (Figure 1b). The structure of the SSU may be further described in terms of a head domain and a body domain. During translation, messenger RNA (mRNA) sequences are decoded by tRNA molecules on the SSU, while the incoming amino acids are added to the growing chain within the peptidyltransferase center of the LSU. The LSU and

SSU each contain three tRNA binding sites, called the aminoacyl (A), peptidyl (P), and exit (E) sites. In order to accurately express a given protein, tRNA molecules sequentially bind and rapidly transit the three binding sites. These processes are controlled by a range of physical processes, including bimolecular association/dissociation events, as well as large-scale conformational changes ($\sim 10-100~\text{Å}$) in the tRNA molecules and ribosomal subunits.

The current study is focused on rotary-like dynamics of the SSU head domain. Structural studies have shown how rotation of the head, a motion known as "head swivel" (Figure 1c,e), can enable the displacement of tRNA molecules between binding sites (i.e., tRNA translocation). However, in addition to this widely recognized form of rotation, simulations have implicated transient rotation about a second axis during translocation, which we will refer to as head tilting. Similarly, normal-mode analysis has shown that tilt-like deformations are energetically accessible. Structural studies have also revealed tilted configurations (Figure 1d,f) that are associated with trans-translation (i.e., a process by which a stalled

Received: August 10, 2022 Revised: October 3, 2022 Published: October 18, 2022





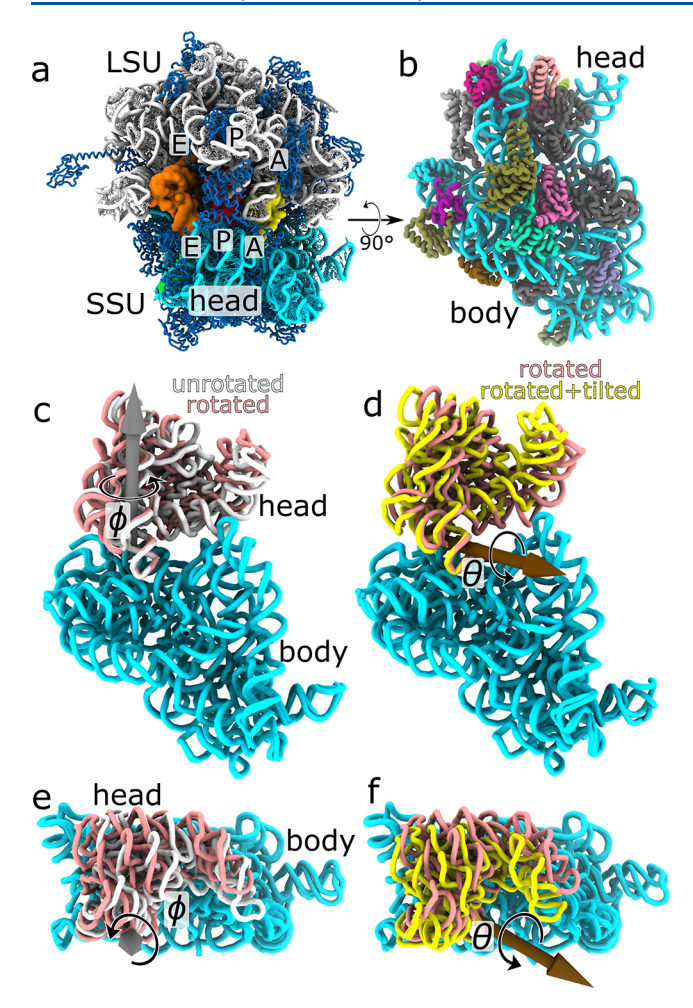


Figure 1. Rotary dynamics in the ribosome. (a) 70S T. thermophilus ribosome structure (RCSB ID: 4V6F⁵¹) showing SSU rRNA (cyan), LSU rRNA (white), ribosomal proteins (blue), and tRNA molecules bound to the A (yellow), P (red), and E (orange) sites of the ribosome. (b) View of the SSU, rotated relative to panel a, with the 20 SSU proteins colored by chain. The current study considers interprotein distances for pairs between the head and body domain of the SSU. (c) Head rotation (i.e., swivel) is described by the angle ϕ , which is defined in terms of motion around an axis that is internal to the rRNA of the head. For reference, the unrotated (white; RCSB ID: 4V4D⁶²) and rotated (pink; RCSB ID: 4V4Q⁶³) orientations are shown, after alignment based on the SSU body (cyan). (d) Head tilting is described by the angle θ , where motion is about a secondary rotation axis. The rotated/untilted structure (pink; RCSB ID: 4V4Q⁶³) and rotated/tilted (yellow; RCSB ID: 7ACR²⁶) are shown, after alignment of the SSU body. (e) Same as panel c, rotated perspective. (f) Same as panel d, rotated perspective. All structural representations were generated with VMD.

ribosome may resume translation), though it is not known if similar motions occurs under typical elongation conditions.

The challenges associated with experimentally isolating specific conformational changes in the ribosome are highlighted by recent molecular dynamics simulations and single-molecule measurements of tRNA translocation. Using an all-atom structure-based model,²⁷ it was shown that steric interactions formed with tRNA molecules can induce head swivel and tilt-like motions.²³ In subsequent smFRET experiments,²⁸ unexpectedly large variations in FRET efficiency were observed, which were interpreted in terms of "exaggerated" head rotation (i.e., swivel). However, despite this

interpretation, the authors noted that head tilting "cannot be ruled out". The reason for this ambiguity is that it is not always possible to use a one-dimensional measure (i.e., smFRET efficiency) to accurately describe a multidimensional process (e.g., rotation and tilting).

It is well-known that the choice of coordinate can profoundly influence the inferred dynamical properties of biomolecules. This has been extensively explored in the context of protein folding, where there is a global orderdisorder transition that occurs in a high-dimensional space. While this is a very complex process, a combination of theoretical and experimental efforts have shown that one can often accurately describe the dynamics in terms of diffusion along a low-dimensional free-energy surface.^{29–32} For example, the number of native contacts can serve as a one-dimensional coordinate that preserves the kinetics of single-domain folding events. 33-36 The end-to-end distance of a protein has also been shown to be an effective coordinate for probing mechanical properties of proteins. ^{37–39} In addition to applying intuitively defined coordinates, general methods have been developed for refining coordinate definitions, such as transition path analysis, 34,40 cut free-energy methods, 41 diffusion map techniques, 42 and variational approaches. 43,44 These many successes in the study of folding have inspired similar efforts for describing conformational motions in the ribosome. For example, transition path analysis has been used to identify suitable coordinates for tRNA rearrangements⁴⁵ and SSU body rotation in the ribosome. 46 Collective variables have also been proposed for quantifying rotation-related motions during translocation.⁴⁷ A direct comparison of projected dynamics along various ribosomal coordinates has also shown how different smFRET labeling strategies can naturally give rise to contradictory inferences.⁴⁸ Similar to studies of folding, these physicochemical analyses are suggesting strategies for precisely describing the energetics of the ribosome.

Here, we aim to resolve the ambiguities associated with interpreting single-molecule measurements of the SSU head domain of the ribosome. Through statistical analysis of interprotein distances, which were obtained from simulations of tRNA translocation on the ribosome, we ask whether one can identify robust measures that are sensitive and specific to head tilting or rotation. This has immediate implications for the interpretation of current single-molecule studies. Further, it demonstrates how multicolor smFRET experiments may be used to simultaneously measure both types of head motion throughout the elongation cycle. Together, this study provides a physically grounded foundation for the design of single-molecule measurements of this prototypical molecular machine.

■ METHODS AND SIMULATION DETAILS

We employed an all-atom structure-based model^{27,49,50} to perform molecular dynamics simulations of mRNA–tRNA translocation in the ribosome. Each simulation (1250, in total) was initiated from the A/P–P/E conformation and terminated when the ribosome reached the classical POST state (P/P–E/E). This data set was used to identify interprotein distances that are sensitive to SSU head rotation and tilting.

Structure-Based Models. For this study, we applied a multibasin all-atom structure-based model of the ribosome that was described by Nguyen and Whitford. First, a crystallographic model of the T. thermophilus ribosome was used to define the pretranslocation state (A/A-P/P) and the post-

translocation state (P/P-E/E). For this, the structure of Jenner et al.⁵¹ (RCSB ID: 4V6F) was used, since it contains tRNA molecules bound to the A, P, and E sites (Figure 1a). The A/ A--P/P model was then defined by removing the E-site tRNA. Similarly, the P/P-E/E conformation was defined by removing the A-site tRNA molecule. Each of these models (A/A-P/P and P/P-E/E) was then used to prepare a singlebasin structure-based model using the SMOG 2 software package.²⁷ All intraribosome interactions were defined based on the classical structure, whereas each tRNA was assigned stabilizing interactions with two binding sites (A and P, or P and E). That is, interactions for each tRNA were defined to stabilize both the pretranslocation and post-translocation conformations. It is important to note that, even though only two structures were used to define the model, energetic competition between the binding sites may lead to the presence of additional local potential energy minima. For a complete description of the energetic model, see Supporting Information.

Simulation Protocols. Simulations were performed using Gromacs v5.1.4.52-55 Reduced units were used for all calculations. Simulations were performed using Langevin dynamics protocols⁵⁶ with a temperature of T = 0.5 (60 Gromacs units). At this temperature, atomic fluctuations are consistent with those inferred from crystallographic Bfactors.⁵⁷ The time step was set to 0.002 reduced units. Each simulation was initiated in an A/P-P/E (hybrid) conformation and terminated when the P/P-E/E (POST) state was reached. The POST state was identified by monitoring distances from both tRNA anticodon stemloops to the P and E sites of the SSU head and body (Figure S1). Each simulation includes a single transition between the hybrid and POST states. The average simulation time per run was roughly 4 × 106 time steps. To interpret the simulated time, we use the estimate that one reduced time unit corresponds roughly to 1 ns, as inferred through a comparison of ribosome simulations performed with structure-based models and explicit-solvent models.⁵⁸ With this time factor, we estimate that each simulation corresponds to $\approx 8 \mu s$.

Analysis. We used the angle ϕ to describe a principal rotation about an axis that is internal to the SSU head (i.e., head swivel; Figure 1c,e). The head tilt angle θ is used to describe any additional rotation that is orthogonal to the principal rotation (Figure 1d,f). We also evaluated the direction of tilting, though it has been shown that the direction is narrowly distributed during tRNA translocation with this model.²³ That is, head tilting predominantly occurs about an axis that is parallel to the bound mRNA. For a complete description of the rotation angles, see SI and Hassan et al.⁸

In order to probe the sensitivity and specificity of interprotein distances to head motions measured by ϕ and θ , we calculated the mutual information between each distance and each head angle. Mutual information was used since it can identify nonlinear dependencies, while also accounting for dispersion in the distance or angle distributions. ^{59,60} Here, we use the standard definition of mutual information:

$$I(a; d) = H(a) - H(a|d)$$

where a is either ϕ or θ and d is a certain SSU interprotein distance. The distribution entropy (H) is given by

$$H(X) = -\sum_{i} P(X = x_i) \ln P(X = x_i)$$

If the mutual information between a distance and an angle is low, one will not be able to reliably infer the angle a from the distance d. However, higher values of I(a;d) would indicate that a given distance may be used to infer the angle. Here we considered the distances between centers of mass of all protein pairs defined by one protein on the SSU head (8, in total) and one on the SSU body (12, in total), for a total of 96 distances. For each interprotein distance, we compared the mutual information with the rotation angle, $I(\phi;d)$, and the mutual information with the tilt angle, $I(\theta;d)$. An interprotein distance is then identified as rotation-specific if $I(\phi;d)$ is much larger than $I(\theta;d)$. Similarly, for tilt-specific distances, $I(\theta;d)$ is larger than $I(\phi;d)$.

In order to quantify how pairs of distances may be used to infer the values of ϕ or θ , the metric $M(a|d_i,d_j)$ is used, which was defined as

$$M(a|d_i, d_i) = H(a) - H(a|d_i, d_i)$$

This metric quantifies the decrease in uncertainty of the value of an angle a, given the values of two distances d_i and d_j . The larger the value of M is, the more precisely the two distances may be used to infer the value of a.

RESULTS

To identify probe sites that may be used in single-molecule experiments to measure SSU head rotation and head tilt, we analyzed the statistical properties of simulated tRNA translocation events. Motivated by recently developed techniques for labeling arbitrary ribosomal proteins, ⁶¹ the current study considers protein—protein distances. We also assess the extent to which available crystallographic and cryo-EM data may be used to identify suitable pairs. Through this, we provide a strategy for the development of next-generation smFRET experiments that may distinguish between head rotation and tilting motions.

Structural Data Suggests Distances That Are Sensitive to Head Motion. To begin our analysis, we will explore the utility of experimental structures for identifying suitable single-molecule probe locations on the ribosome. For this, we adopt the strategy that is typical when designing singlemolecule experiments, where probe locations are selected based on maximal differences in representative structures. To this end, we analyzed all published structures of E. coli ribosomes (365 complete ribosomes, see Appendix). Of these, we selected five structures^{26,62-65} that span the range of tilt and rotation angles for the head (Figure 2). One structure (RCSB ID: 7ACR) exhibits the largest value for the head tilt angle ($\theta = 12.6^{\circ}$). The other four ribosomes [RCSB IDs (rRNA chains): 4V9D (DA, BA), 4V4Q (DB, CA), 7SS9 (1, 3), 7D80 (A, B)] are associated with unrotated ($\phi = 0^{\circ}$, -1.9°) or highly rotated ($\phi = 19.5^{\circ}$, 14.9°) head domains, and small tilt angles ($<4.0^{\circ}$). If the distance between the geometric centers of protein i and j, denoted $d_{i,i}$ is considerably larger $(\sim 5 \text{ Å})$ in the head-tilted ribosome than in the untilted structures, then it is possible that the protein pair may represent a suitable candidate for use in single-molecule experiments. Further, if the distance $d_{i,j}$ has a small range of values ($\delta d_{i,i}$ < 5 Å) within the four untilted ribosomes, then it may represent a tilt-specific measure.

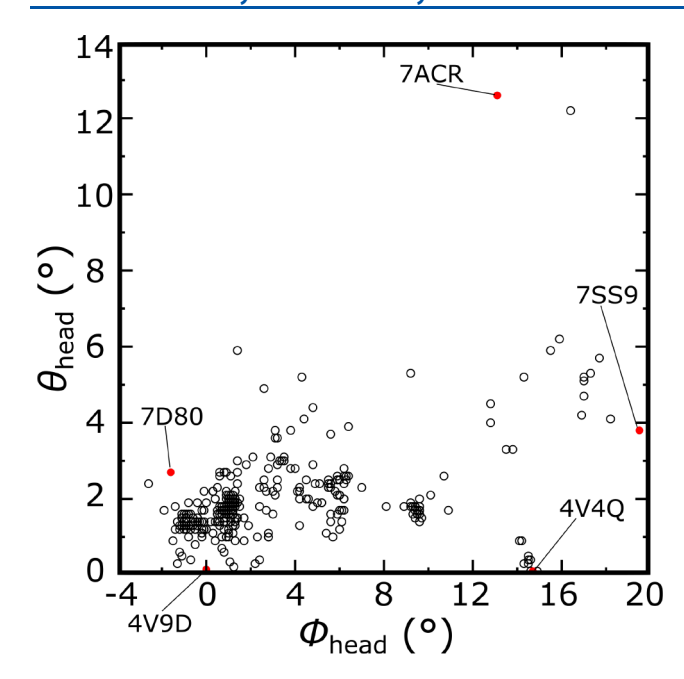


Figure 2. SSU head rotation and tilt angle from experimental structures. To initiate our investigation of suitable measures to describe head motions, we evaluated the rotation and tilt angles for all published structures of *E. coli* 70S ribosomes (365 structures). There is a dense population of nonrotated structures (ϕ < 5°) that include pre- and post-translocation states. A few structures also exhibit large-scale tilting displacements of the head. From this set, we used five representative structures (red circles; labeled by RCSB ID) for comparative analysis.

Among all interprotein distances considered, six appear to be specific to head tilting (Table S1). As an example, $d_{S10,S12}$ is nearly identical (93-94 Å) in all four nontilted structures. However, it is significantly larger (101 Å) in the head-tilted structure. This would suggest that proteins S10 and S12 may be used in experiments to specifically detect head tilting. To further assess this pair, we calculated the range of distances $(\delta d_{\rm S10,S12})$ from all 345 structures for which tilting is minimal $(\theta < 4^{\circ})$. Unfortunately, this reveals that the range of distances within the untilted ensemble of structures (11.7 Å) is larger than the difference between the representative tilted and untilted structures (~8Å). Accordingly, these comparisons suggest that it could be difficult to discern whether changes in experimental measurements are due to tilting, or rotation. We find similar limitations for the other five candidate distances identified from this comparative approach. Together, analyzing hundreds of structures highlights how the choice of representative structures can bias the potential interpretation of single-molecule measurements.

Single-Molecule Measurements Corroborate Predicted Tilting Motion. We next analyzed the statistical properties of simulated tRNA translocation trajectories. To assess the utility of the simulated data set, we first compare the predicted dynamics with independently reported single-molecule measurements. In these simulations, we employ the same model and protocols described by Nguyen and Whitford.²³ Since the experimental study²⁸ was published after the previous set of simulations, the presented comparison serves as an unbiased assessment of the predictive capabilities of the model. As detailed below, we find broad agreement between the simulations and experimental measures, which suggests our simplified model is sufficiently complete that it

can provide a suitable approximation to the balance between SSU head motions during translocation.

In the current study, we consider molecular dynamics simulations of tRNA translocation, which were generated using an all-atom multibasin structure-based (SMOG) model.²⁷ In each simulation, the ribosome transitions from a so-called "hybrid" state, where the tRNA molecules bridge multiple binding sites on the ribosome, to the "POST" (P/P-E/E)state. This data set includes 1250 simulated translocation events (250 reported previously, 23 along with 1000 additional simulations). During each simulation, there is transient and spontaneous (i.e., without use of steering or targeting protocols) rotation ($\sim 15-20^{\circ}$) and tilting ($\sim 10-15^{\circ}$) of the SSU head. In this model, the pre- and post-translocation (i.e., unrotated and untilted) conformations are explicitly defined to be potential energy minima.²³ While this is an intentionally simplified description, the SMOG model accounts for molecular sterics, and the modeled flexibility of the ribosome is consistent with crystallographic B-factors. Accordingly, the observation of spontaneous rotation/tilting shows how the atomic excluded volume can induce large-scale rearrangements of the SSU head during tRNA translocation. Since the predicted timing and scale of SSU motions are dictated by the structure of the ribosome, this description may be considered a physically grounded lowest-order approximation of the dynamics. As described in detail previously, 23 this model shows that the biomolecular structure predisposes the SSU and tRNA molecules to undergo a clear sequence of conformational rearrangements (Figures 3 and 4 of ref 23). In each simulation, the SSU head is initially rotated by roughly 5°. During tRNA translocation, the SSU head spontaneously rotates to larger values ($\phi \approx 15-20^{\circ}$; Figure 3c and Figure S2a). Head rotation is then followed by a secondary orthogonal rotation (i.e., head tilting) that is generally about an axis parallel to the mRNA (Figure 1d,f). Tilting motion is described by the angle θ , which reaches values of 8–15° during the simulated events (Figure 3e and Figure S2a). In order to complete the translocation process, the SSU head then returns to the unrotated/untilted conformation.

We find that independently reported single-molecule measurements are consistent with the presence of SSU head tilting during the late stages of tRNA translocation. Specifically, the dynamics predicted by the SMOG model and singlemolecule measurements of Wasserman et al.28 exhibit fluctuations that are similar in scale. In the single-molecule study, two labeling strategies were deployed to specifically follow the motion of the SSU head. The first labeling pair is protein S13 (on the SSU) and protein L5 (on the LSU; Figure 3a). The second pair is protein S13 and the elbow of the P-site tRNA (which transitions to the E site during translocation). For both of these FRET pairs, the authors observed anomalous fluctuations that immediately preceded the adoption of a posttranslocation state (POST). Since these fluctuations exceeded the values assigned to the fully rotated head configuration, they were described as signifying "exaggerated" head rotation motions that likely represented large-scale rotation/swivel. However, since the FRET signals were one-dimensional measures, the authors noted that it is possible that other forms of rotation (e.g., tilting) could also explain these fluctuations.

In the first set of experiments, Wasserman et al. monitored the proteins S13 and L5. In their experiments (Figure 6 of ref 28), the FRET efficiency (*E*) was initially at an intermediate

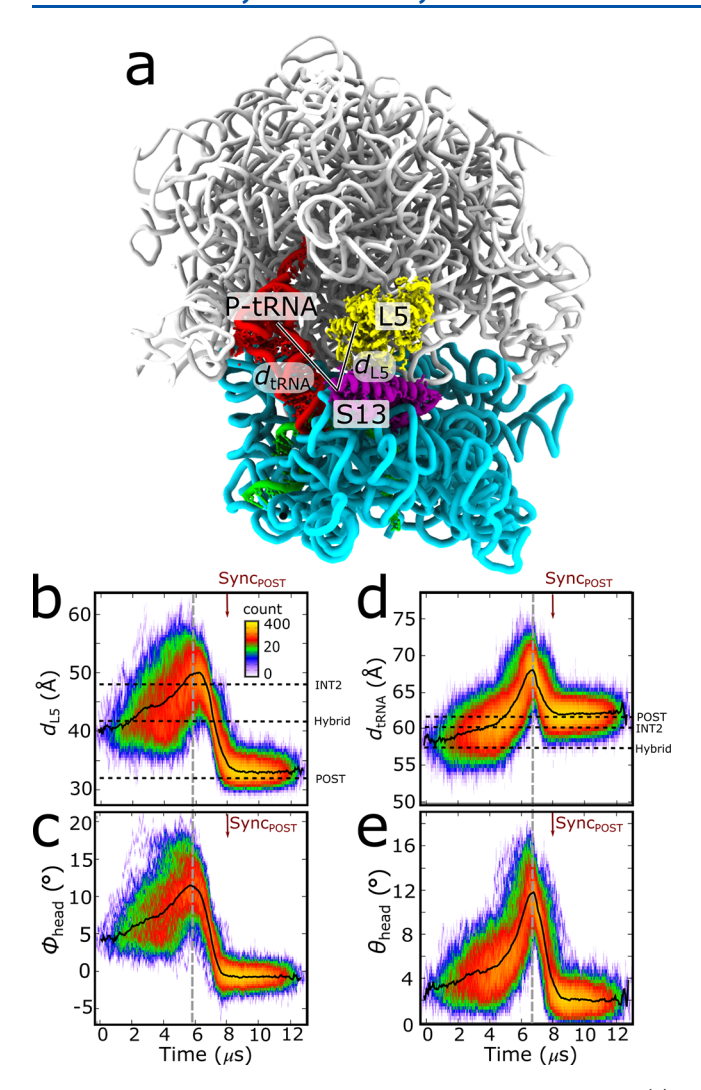


Figure 3. Predicted motions are similar to smFRET observations. (a) To probe SSU head motions in single-molecule FRET experiments, Wasserman et al.²⁸ introduced FRET pairs on proteins S13 and L5, as well as S13 and the P-site tRNA molecule. (b) Postsynchronized time traces for the distance between probe sites on S13 and L5 (d_{L5}), calculated from simulations. For reference, the values corresponding to INT2 (RCSB IDs: 4V9L, 4V9M⁶⁶), a pretranslocation hybrid conformation (RCSB ID: 4V9H⁷⁵), and a unrotated structure (POST; RCSB ID: 4V6F⁵¹) are shown. Consistent with smFRET observations, the distance is found to transiently exceed the value found in the INT2 structures. (c) Postsynchronized time traces for the head rotation angle ϕ . The simulations suggest a correlation between the S13-L5 distance and the rotation angle ϕ . (d) Postsynchronized time traces for the distance between S13 and the P-site tRNA (d_{tRNA}). Consistent with observations of Wasserman et al., we find a transient increase in distance immediately before completing the translocation process. (e) Postsynchronized time traces for the head tilt angle θ . The S13-tRNA distance is visibly correlated with θ .

value (E=0.55), which was biochemically assigned to correspond to a rotated body domain with tRNA molecules in hybrid configurations. Upon the addition of elongation factor-G(GTP) (EF-G: a GTPase that facilitates tRNA translocation on the ribosome), the S13–L5 signal showed a decrease (E=0.4) before a large increase to reach the value corresponding to the POST structure (E=0.75). For reference, E is roughly 0.5 when the head-rotated configuration

is trapped in a pretranslocation intermediate (referred to as INT2 by Wasserman et al.²⁸) through the introduction of fusidic acid. Thus, values lower than 0.5 would signify largerscale rotation, or alternate forms of SSU head motion. To compare with these observations, we calculated d_{L5} : the distance between the residues (distance between C_{α} atoms) labeled in S13 and L5. We then postsynchronized our simulated events in a manner consistent with the experimental study (Figure 3b-e). Specifically, we aligned all trajectories in time, such that the POST state is reached at $t = Sync_{POST}$. In our simulations, $d_{\rm L5}$ initially samples values that are approximately 41 Å, which is consistent with the value found in a cryo-EM reconstruction of a pretranslocation (hybrid) intermediate (Figure 3b). Next, d_{L5} increases to ≈ 50 Å and then decreases to \approx 32 Å, which is very close to the value found in the classical POST structure (31 Å). Consistent with the single-molecule observations, d_{L5} is found to transiently exceed the values found in the putative fully rotated conformation (i.e., INT2, corresponding to RCSB IDs: 4V9L, 4V9M⁶⁶). This change in d_{LS} is also visibly correlated with a large increase in ϕ , which reaches values of $\approx 10^{\circ} - 20^{\circ}$ before returning to $\approx 0^{\circ}$ in the POST state (Figure 3c). While this suggests that S13-L5 probes are sensitive to rotation, the simulations indicate that the anomalous experimental fluctuations may arise without a need for the SSU head to adopt more highly rotated (e.g., in excess of $\sim 20^{\circ}$) configurations.

In the second set of experiments, FRET probes were placed on protein S13 and the elbow of the P-site tRNA molecule. The corresponding signal (SI Figure 7 of ref 28) was found to start from a high FRET state (E = 0.8). Upon addition of EF-G(GTP), the FRET signal decreased to approximately 0.55 before increasing to ~0.65. As noted above, this transient "dip" to 0.55 suggested the presence of a rearrangement in the head that immediately precedes completion of translocation. In the simulations, we analyzed the distance between the corresponding labeled residues (d_{tRNA}) and postsynchronized the traces based on the time at which the POST state was adopted. Consistent with the experimental observations, the model predicts that d_{tRNA} initially increases from \approx 58 Å to 70 Å and then decreases to the POST value (\approx 62 Å; Figure 3d). In contrast to the interpretation of Wasserman, we find that changes in d_{tRNA} coincide with transient large-scale tilting of the head ($\theta \approx 12^{\circ}$, Figure 3e). Overall, these comparisons show that the range of motions predicted by the SMOG model are consistent with those observed in single-molecule experiments, though the simulations implicate tilting motions, which differs from the interpretation suggested in the experimental report.

Identifying Rotation-Specific and Tilt-Specific Measures. Since our simulated data set includes rotation and tilt-like motions that are consistent with experimental observations, we next used our trajectories to identify interprotein distances that are sensitive and specific to each motion. We first examined two-dimensional probability distributions, calculated with respect to a distance $(d_{i,j})$ and angle (ϕ) , or θ . Based on visual inspection, several classes of relationships were apparent, including highly nonlinear associations (see Figure S3). Since it is possible that nonlinear relationships may be exploited in the design of single-molecule experiments, we calculated the mutual information (MI) between each interdomain distance and each SSU head angle (ϕ) and (ϕ) . In contrast to Pearson correlation coefficients, MI may be used to identify linear, or nonlinear, relationships between arbitrary

variables. Here, we use the symbol $I(\phi; d)$ to denote the mutual information between an interprotein distance *d* and the head rotation angle ϕ . We defined the MI with tilting angle θ analogously. For both calculations, MI was evaluated from all simulated frames that are associated with an active transition between the hybrid and POST state. That is, sampling of the hybrid state at the beginning of each simulation, and extended sampling of POST at the end, were excluded. If the angle a (i.e., ϕ or θ) is independent of d, then I(a; d) = 0. On the other hand, if there is any functional dependence (linear or nonlinear) between a and d (indicating sensitivity of this distance to a particular head motion), then I(a; d) will be nonzero, where larger values of I(a; d) indicate stronger dependencies. This allows MI to identify distances that are sensitive to head rotation or head tilting, irrespective of the functional relationship. Furthermore, since all functional relationships are described, MI allows us to apply a stringent criterion for quantifying specificity.

To identify distances that are specific to SSU head rotation, we compared the values of $I(\phi; d)$ and $I(\theta; d)$. We then defined a specificity factor as $S_d^{\phi} = \frac{I(\phi; d)}{I(\theta; d)}$. If $S_d^{\phi} > 1$, the distance d is more specific to head rotation, where larger values indicate a higher level of specificity. Distances that exhibit large values of S_d^{ϕ} are expected to be suitable for specifically monitoring head rotation. We defined an analogous specificity measure for tilting: $S_d^\theta = \frac{1}{S_d^\phi} = \frac{I(\theta;d)}{I(\phi;d)}$. The calculated values of mutual information for all interdomain protein distances d with both ϕ and θ angles are shown in Figure 4. Of the 96 distances considered, we found that 42 distances are associated with small mutual information with both ϕ and θ . Even though these are interdomain distances, they would not be suitable for experimentally following head dynamics, since they are not sufficiently sensitive to either type of head motion. Of the remaining protein pairs, 26 are specifically sensitive to head rotation ($S_d^{\phi} > 3$; Table S2). We also found 7 pairs that are more specific and sensitive to head tilting ($S_d^{\theta} > 3$; Table S3).

Structural considerations can help explain why specific protein pairs are identified as suitable candidates to monitor head motion. For this discussion, we will focus on example distances that are less than 10 nm, since longer ranges are not typically accessible in most smFRET applications. As a first example, $d_{S2,S7}$ (Figure 5a) is informative about head rotation $(I(\phi; d) = 0.70$, see Figure 5b) and negligibly informative about head tilting ($I(\theta; d) = 0.09$, see Figure 5d). It is the most specific shorter-range distance (<10nm) for head rotation, where $S_d^{\phi} = 7.37$. In the simulations, the mean value of $d_{S2,S7}$ is 75 Å, and we find the distance varies approximately linearly with ϕ , where the slope of a linear fit is -0.4 Å per degree (Figure 5b). This strong relationship between distance and rotation angle suggests that appreciable changes in FRET would require changes in rotation of $\sim 10^{\circ}$. As noted above, these distances are calculated based on the centers of mass of the proteins. Accordingly, there are numerous pairs of residues between these proteins that are associated with shorter distances, which may be a desirable property when designing new experimental applications. In terms of structural properties, the vector between S2 and S7 is roughly perpendicular to the axis of rotation (Figure 5a), which rationalizes the observed sensitivity to rotation. This vector is also roughly parallel to the axis of tilting, which rationalizes the insensitivity to tilting. As

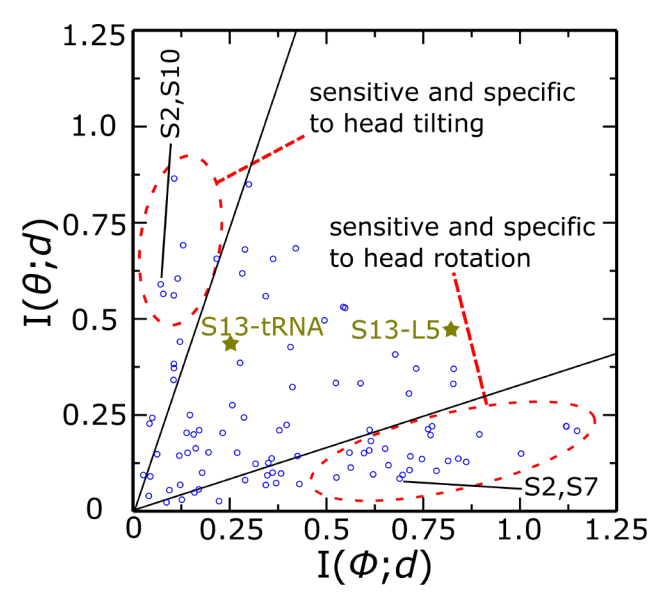


Figure 4. Identifying distances sensitive and specific to particular forms of head motion. To identify quantitative relationships between interprotein distances and rotations, we calculated the mutual information between a given distance d and each angle $(I(\phi; d), I(\theta; d))$. Distances with large $I(\phi; d)$ and small $I(\theta; d)$ (bottom right) are sensitive and specific to head rotation. The horizontally oriented line indicates $S_d^{\phi} = \frac{I(\phi; d)}{I(\theta; d)} = 3$. Distances with large $I(\theta; d)$ and small $I(\phi; d)$ (top left) are sensitive and specific to head tilting. A line is shown for $S_d^{\theta} = \frac{I(\theta; d)}{I(\phi; d)} = 3$. Many distances are insensitive or nonspecific to one form of head motion. For comparison, the distances probed by Wasserman et al. are labeled "S13–L5" and "S13–tRNA".

another example, $d_{S2.S10}$ (Figure 5a) is sensitive to head tilting $(I(\theta; d) = 0.59$, see Figure 5e) and not sensitive to head rotation $(I(\phi; d) = 0.07, \text{ see Figure 5c})$. This is the most tilting-specific distance, where $S_{S2-S10}^{\bar{\theta}}=8.24$. In the simulations, $d_{S2,S10}$ has a mean of 77 Å with a change of -0.4 Å per degree of tilting (Figure 5e). Accordingly, S2 and S10 represents a promising pair for precisely monitoring head tilting. In terms of ribosome structure, the interprotein vector formed by these proteins is roughly parallel to the head rotation axis (Figure 5a), suggesting it may be suitable for monitoring orthogonal degrees of freedom, such as tilting. In general, for pair distances that have a large S_d^{θ} value, the corresponding interprotein vectors are generally found to be parallel to the rotation axis. For a complete list of protein pairs and specificity factors, see Tables S2 and S3. To relate these quantities to current experimental practices, it is interesting to note that these pairs were significantly more specific to rotation and tilting than those used by Wasserman et al. (Figure 3a, see stars in Figure 4).

Approaches to Simultaneously Measure Rotation and Tilt. We will conclude our analysis by considering possible applications of multicolor FRET experiments to resolve the precise orientation of the ribosome. Specifically, we will focus on the potential for three-color smFRET experiments (i.e., two distances) to simultaneously probe the rotation and tilt angles of the SSU head domain. While current multicolor methods may not have sufficient time resolution to make such precise inferences, this analysis aims to provide a guide with which next-generation experiments may

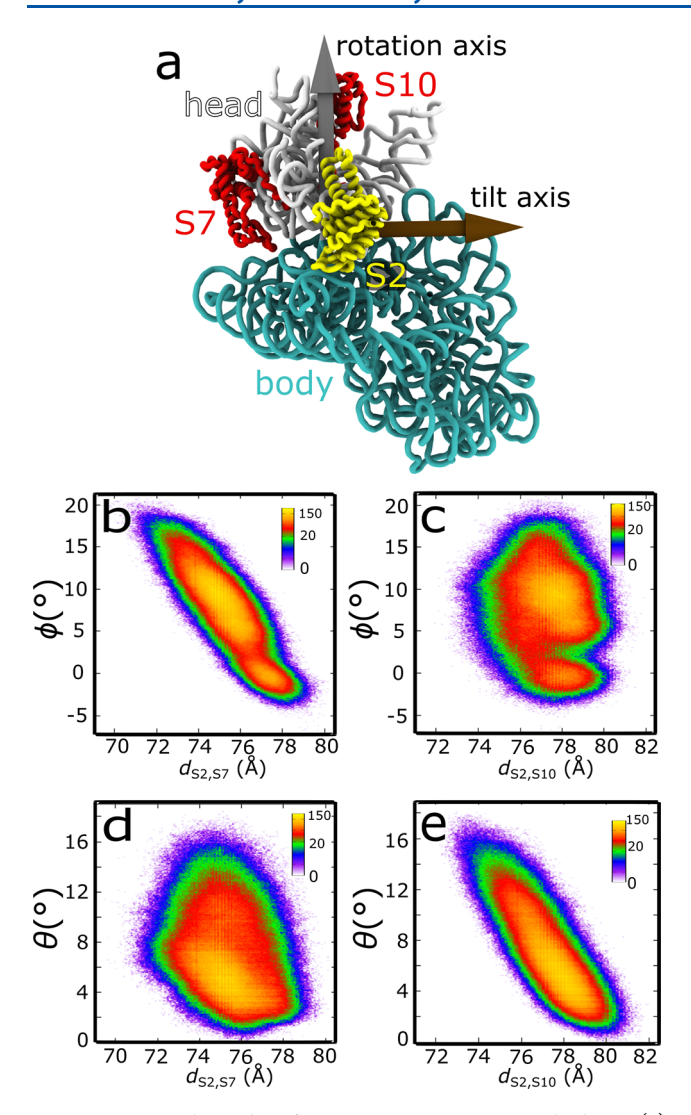


Figure 5. Example probes for monitoring rotation and tilting. (a) Structure of a T. thermophilus SSU with protein S2, S7, and S10 shown. The distance between proteins S2 and S7 $(d_{S2,S7})$ shows sensitivity and specificity with ϕ , but not with θ . The proteins are roughly aligned perpendicular to the rotation axis and parallel to the tilt axis. In contrast, the distance between proteins S2 and S10 $(d_{S2,S10})$ is sensitive and specific to θ , but not ϕ . This insensitivity to rotation is consistent with these proteins being roughly aligned along the rotation axis. (b) 2D histogram showing the relationship between $d_{S2,S7}$ and ϕ . (c) Distribution of $d_{S2,S10}$ and ϕ . (d) Distribution of $d_{S2,S7}$ and ϕ . The S2–S7 pair can be used to specifically monitor head rotation during translocation. (e) 2D histogram showing the relationship between $d_{S2,S10}$ and ϕ . The S2–S10 pair can be used to specifically monitor head tilting during translocation.

dissect the complex interplay of rotation and tilting. It is important to mention that the ability to measure the orientation of the SSU head based on only two metrics is not guaranteed. That is, even if one were to assume the SSU head moves as a rigid body, the orientation will still be associated with three degrees of freedom. Despite this, we find that some combinations of two interprotein distances are sufficient to unambiguously assign simultaneous values to ϕ and θ . Technically, one could also use measurements from multiple two-color FRET experiments. However, as described elsewhere, 67,68 such efforts would only be reliable if the FRET

states in different experiments could be definitively assigned to the same physical state of the ribosome.

In order to examine how simultaneously measuring two distances could enable one to infer the values of ϕ and θ , we defined the quantity $M(a|d_i, d_i) = H(a) - H(a|d_i, d_i)$. This quantity measures the decrease of uncertainty in the value of the angle a (either ϕ or θ), given the value of two distances. This metric carries the benefits of MI, while enabling one to systematically identify which pairs of distances yield the largest amount of information about the head orientation. To compare between different pairs of interdomain distances, we considered the metric $M(a|d_i, d_i)$ for all possible pairs of interdomain distances d_1 and d_2 (Figure 6a,b). We will limit the discussion to sets of pairs that contain a common protein. This condition is imposed in order for the current analysis to be amenable to three-color FRET experiments. Of all considered pairs, the most promising candidates are those that exhibited large values for $M(\phi|d_i, d_i)$ and $M(\theta|d_i, d_i)$ (Figure 6a,b). For eight distance pairs, we find that both metrics are greater than 1.3 (Table S4). Accordingly, this analysis identifies a small set of protein triplets that may be used to simultaneously probe the rotation and tilt angles of the SSU head.

To provide an illustrative example for how two distances may be used to infer rotation and tilt, we will consider $d_{S11,S19}$ and $d_{S12,S19}$. $d_{S12,S19}$ does not yield exceptionally large mutual information values for ϕ or $\theta(I(\phi; d_{S12,S19}) = 0.55, I(\bar{\theta}; d_{S12,S19})$ = 0.53), suggesting that this distance is not particularly useful when used alone. However, interestingly, this pair of distances shows high M values for both ϕ and θ , indicating they may be used together to obtain insights into the simultaneous values of both angles. To demonstrate how these distances may be used to differentiate between predominantly rotated and predominantly tilted orientations, we calculated the conditional probability P(a|R), where a is either ϕ or θ , and R denotes a region of configuration space defined by the two coordinates. First, we considered the region R to be defined as 9.3 nm $< d_{S11,S19} < 9.6$ and 9.0 nm $< d_{S12,S19} < 9.3$ nm. For these values of the distances, ϕ is distributed around 2°, while $\theta \approx 12^\circ$ (Figure 6c,d), which corresponds to a predominantly tilted ensemble. In contrast, when the region R is defined as 10.8 nm <d_{S11.S19}< 11.1 nm and 9.0 nm <d_{S12.S19}< 9.3 nm, then $\phi \approx$ 15° and $\theta \approx 5^\circ$, corresponding to predominantly rotated configurations (Figure 6e,f). Taking this further, we also find that these two distances may be used to simultaneously infer reliable estimates of ϕ and θ throughout the translocation process. For this, we performed a multilinear least-squares regression analysis for head angles with $d_{S11,S19}$ and $d_{S12,S19}$. The best fit provides a quantitative relation between the two distances and two angles (distances are in nm and angles in degrees):

$$\phi = -9.82d_{S11,S19} + 4.17d_{S12,S19} + 71.36$$

$$\theta = 5.82d_{S11,S19} + 7.95d_{S12,S19} - 124.16$$

This multilinear least-squares regression is an accepted model for the dependence of ϕ and θ on $d_{S11-S19}$ and $d_{S12-S19}$, as suggested by examining the covariance matrix of the regression coefficients (see Table S5). Since the two distances are defined by a protein triplet, this shows how three dyes could be used in a multicolor smFRET experiment to

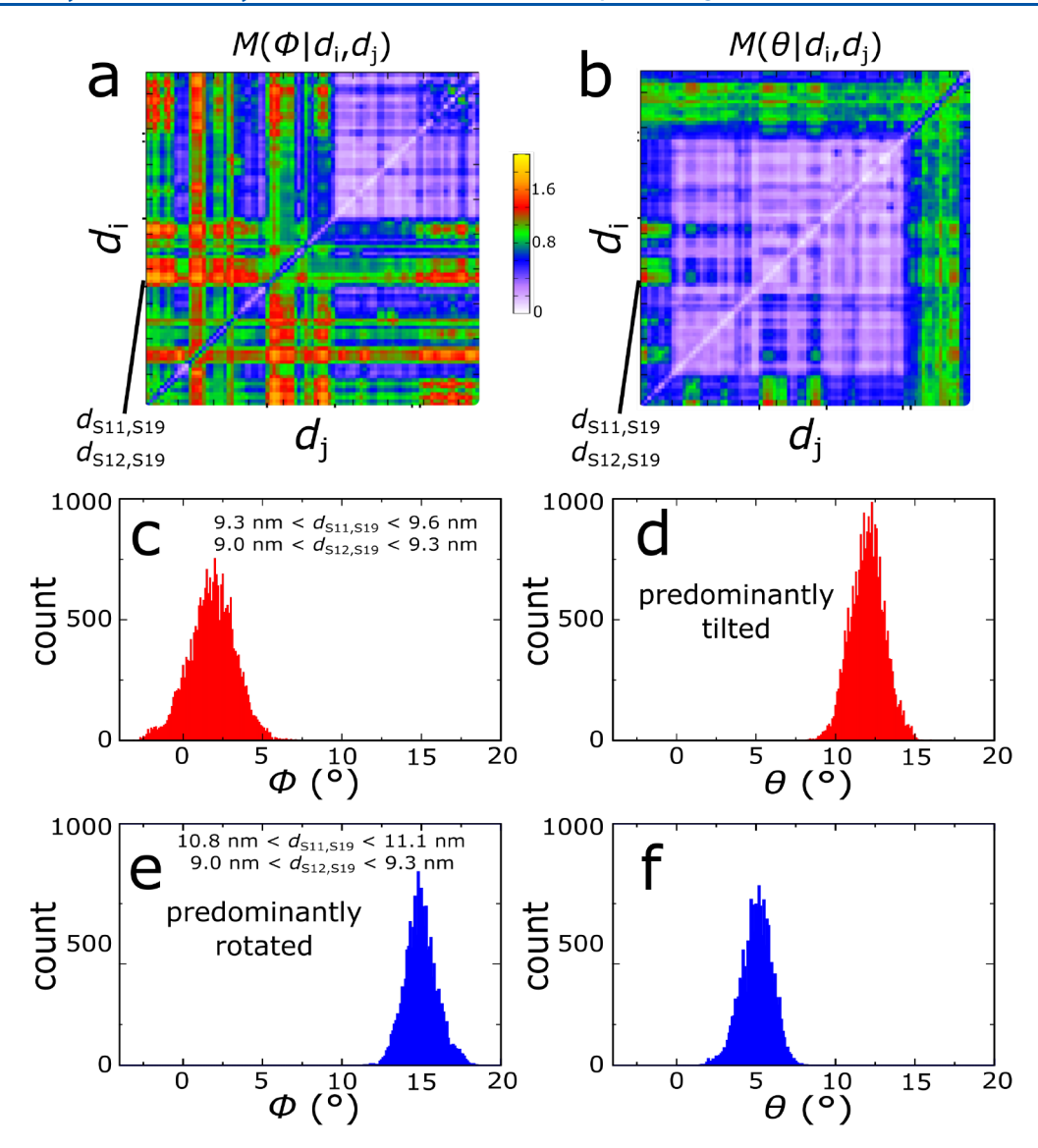


Figure 6. Complete determination of SSU head orientations. To quantify the precision with which rotation or tilt may be inferred based on knowledge of two distances $(d_i \text{ and } d_j)$, the metric $M(a|d_v d_j) = H(a) - H(a|d_v d_j)$ was applied (a is an angle). High values indicate that two distances may be used to precisely determine the angle. In contrast to mutual information measures (Figure 4), a large value of M for both ϕ and θ would indicate the pair may be used to distinguish between the two types of rotation. (a) $M(\phi|d_v d_j)$ for all combinations of distances. (b) $M(\theta|d_v d_j)$ for all combinations of distances. Some pairs of distances show large M values for both angles, indicating they may be used to define accurate least-squares regression models (see Results section). (c, d) Conditional probability distributions (unnormalized) when $d_i \equiv d_{S11,S19}$ and $d_j \equiv d_{S12,S19}$ are known. For the first ranges of $d_{S11,S19}$ and $d_{S12,S19}$ (panels c and d), one could infer that the head is tilted and unrotated. Conversely, for a second range of values (panels e and f), one could precisely infer that the head is rotated and marginally tilted. For a 2D heatmap showing these populations of head orientations conditioned on distance values, see Figure S6.

simultaneously monitor SSU head rotation and tilting during translocation.

DISCUSSION AND CONCLUSIONS

Quantifying Energetics of Large-Scale Assemblies.

The current study makes an effort to establish quantitative relationships between possible experimental measurements and specific motions of interest in the ribosome. While decades of biochemical and structural analysis have revealed a broad range of subunit orientations in the ribosome, the precise relationship between rearrangements in the ribosome and functional dynamics of tRNA molecules is still an active area of investigation. In the case of SSU head rotation, cryo-EM and X-ray crystallography studies have shown that changes in head rotation are associated with the adoption of so-called hybrid

tRNA configurations. While such correlations implicate an energetic relationship between tRNA molecules and the ribosome, the nature of this association has yet to be quantified.

In terms of the physicochemical properties of elongation, one may envision a number of ways in which the free-energy landscape of a tRNA molecule may depend on the orientation of the ribosomal subunits. First, there may be weak energetic coupling between the tRNA molecules and the subunits, where the landscape of the tRNA is only marginally influenced ($\sim k_{\rm B}T$ scales) by subunit rotation. An alternate scenario would be that a large free-energy barrier (>10 $k_{\rm B}T$) is associated with movement of the tRNA, where the barrier abruptly reduces in scale once the ribosome has reached a critical rotation state. Yet another possibility is that each tRNA molecule has a free-

energy minimum that is monotonically displaced as the subunit rotates. Each of these relationships represents a plausible proposal, though determining which physicochemical mechanism is applied will rest on the ability to reliably monitor and describe the orientations of the subunits.

Through the analysis of simulated tRNA translocation trajectories, we provide a statistical foundation that will allow the field to precisely monitor the orientation of the SSU head domain. After considering 96 potential protein pairs that may be labeled in experiments, we find that 33 appear to be promising. These measures are sensitive and specific to either head rotation, or head tilting. If one were to probe these sites experimentally, then the presented analysis would serve as a physical basis for directly interpreting the structural significance of a given signal. Thus, through this form of analysis, future experiments may soon be able to precisely quantify the dynamical relationships of the many molecular components of this assembly.

Opportunities and Challenges. To conclude our discussion, it is important to briefly discuss some remaining challenges in the development of next-generation single-molecule methods. These obstacles may require novel theoretical developments, as well as strategies to overcome practical experimental limitations.

In terms of theoretical challenges, there are two notable steps that should be pursued in the immediate future. First, the current study focused on the separation of the centers of mass of proteins. Since smFRET experiments label individual residues, and not the center of mass, additional analysis could help further guide the placement of novel probes. In this direction, it is important to note that the radius of a typical SSU ribosomal protein is roughly 2 nm, whereas the interprotein distances considered here are generally significantly longer. In addition, ribosomal proteins remain folded and ribosome-bound during subunit rotation. Accordingly, it is expected that during head rotation most residue-residue distances will be strongly correlated with the associated centerof-mass distances. However, even though the current analysis does not implicate specific residue pairs, it provides an intuitive strategy for identifying promising labeling sites. That is, residue pairs that are aligned parallel to the rotation axis are generally expected to be more sensitive to tilting, while those that are parallel to the tilting axes should be more sensitive to rotation. To systematically consider and assess specific residue pairs, one could consider expanding the analysis to include all residueresidue pairs. However, with the large number of protein residues in the ribosome, direct evaluation of all coordinates would rapidly become computationally intractable. As an alternate, analytical approaches that employ rigid-body approximations may be sufficiently accurate that one could reliably identify and sort the effects of labeling position within a protein. Such an effort could provide a smaller set of promising residue pairs, which could then allow for more rigorous characterization of dyes and labeling sites (e.g., simulation-based modeling approaches to quantify dye mobility⁶⁹).

Another potential theoretical limitation is the choice of model that is used to generate representative trajectories of a given process. Here, we used an all-atom model with simplified energetics (i.e., structure-based "SMOG" model). In this model, the energetics of the tRNA molecules are approximated as only having attractive interactions with the ribosomal binding sites. Thus, the relationship between tRNA and the

SSU head is steric in nature. While this provides an appropriate first approximation, the most notable omission in this model is the lack of electrostatic interactions. To address this, a SMOG model variant was recently presented that includes explicit electrostatics and diffuse ions. 70 In that specific study, the process of aa-tRNA accommodation was simulated, where the tRNA molecule spontaneously associates and dissociates with the ribosomal A site. Those calculations showed that, even though the free-energy barrier was very sensitive to the ionic composition, the overall mechanistic/structural properties were robust. That is, the sequence of conformational steps was similar when explicit ions were included, or when electrostatics and ions were excluded. Given the strong steric relationship between tRNA motion and SSU head rotation, it is reasonable to anticipate a similar level of robustness in the dynamics of translocation. Thus, while the current model is not energetically complete, one expects that the study of coordinates will not depend strongly on the choice of model.

In terms of experimental methods, the most prominent challenge is that ideal probe locations are not always biochemically accessible. That is, one must select sites that will not perturb the assembly and functional dynamics of the biomolecular complex. Fortunately, recent biochemical techniques presented by Desai and Gonzalez⁶¹ largely mitigate this issue for the ribosome. In their protocol, one can encode noncanonical amino acids in almost any ribosomal protein, and a dye is then ligated to the mutated residue. In their proof-ofprinciple application, they labeled eight different proteins on the SSU (S5, S6, S7, S11, S12, S13, S18, and S19). In our analysis, we find that many combinations of these proteins can be suitable for specifically monitoring head rotation. However, none of the identified tilt-specific measures are formed by pairs of proteins from this experimentally probed set. Accordingly, introducing dyes to a specific set of additional proteins may be sufficient to decipher the balance between rotation and tilting in experiments.

Another opportunity for advancing single-molecule studies of the ribosome involves accessing longer distances. While we find interprotein pairs that are specific to rotation or tilting, many of the highly ranked pairs are associated with distances that exceed 100 Å, which would not be viable for most smFRET experiments. To address this, there are ongoing efforts to improve the use of zero-mode waveguides (ZMWs) to provide enhanced signals at distances well beyond this range for model systems. In addition, there is a history of successful applications of ZMW technology in smFRET experiments of the ribosome. While there may be technical challenges associated with implementing ZMW methods to access longer distances in the ribosome, our analysis provides a motivation to pursue such efforts.

CONCLUSIONS

Studies at the interface of theory and experimentation have proven to be extremely effective at enabling physically guided molecular-level experiments. In addition, this synergy has provided much needed quantitative assessments of molecular processes, which have allowed for further refinement of theoretical concepts. For the ribosome, a similar opportunity is beginning to arise from a combination of innovative single-molecule methods and advances in theoretical techniques. The current study serves to highlight the utility of theoretical models by providing a guide for developing next-generation single-molecule experiments. We also present an example

where current single-molecule methods provide a valuable point of comparison, upon which theoretical models may continue to be refined. It is our expectation that similar comparisons will increase in frequency, which will ultimately allow for an experimentally grounded physicochemical description of the ribosome to emerge.

ASSOCIATED CONTENT

Supporting Information

The Supporting Information is available free of charge at https://pubs.acs.org/doi/10.1021/acs.jpcb.2c05706.

Supporting methods, and tables and figures containing additional results (PDF)

Appendix containing information about all published *E. coli* ribosomes (365) used in analysis in Figure 2 (TXT)

AUTHOR INFORMATION

Corresponding Author

Paul C. Whitford — Department of Physics, Northeastern University, Boston, Massachusetts 02115, United States; Center for Theoretical Biological Physics, Northeastern University, Boston, Massachusetts 02115, United States; orcid.org/0000-0001-7104-2265; Email: p.whitford@northeastern.edu

Author

Asem Hassan — Department of Physics, Northeastern University, Boston, Massachusetts 02115, United States; Center for Theoretical Biological Physics, Northeastern University, Boston, Massachusetts 02115, United States

Complete contact information is available at: https://pubs.acs.org/10.1021/acs.jpcb.2c05706

Notes

The authors declare no competing financial interest.

ACKNOWLEDGMENTS

P.C.W. was supported by NSF grant MCB-1915843. Work at the Center for Theoretical Biological Physics was also supported by the NSF (Grant PHY-2019745). We acknowledge generous support provided Northeastern University Discovery Cluster.

REFERENCES

- (1) Harms, J.; Schluenzen, F.; Zarivach, R.; Bashan, A.; Gat, S.; Agmon, I.; Bartels, H.; Franceschi, F.; Yonath, A. High resolution structure of the large ribosomal subunit from a mesophilic Eubacterium. *CELL* **2001**, *107*, 679–688.
- (2) Carter, A.; Clemons, W.; Brodersen, D.; Morgan-Warren, R.; Wimberly, B.; Ramakrishnan, V. Functional insights from the structure of the 30S ribosomal subunit and its interactions with antibiotics. *Nature* **2000**, *407*, 340–348.
- (3) Ban, N.; Nissen, P.; Hansen, J.; Moore, P.; Steitz, T. The complete atomic structure of the large ribosomal subunit at 2.4 angstrom resolution. *Science* **2000**, 289, 905–920.
- (4) Yusupov, M. M.; Yusupova, G. Z.; Baucom, A.; Lieberman, K.; Earnest, T. N.; Cate, J. H.; Noller, H. F. Crystal structure of the ribosome at 5.5 A resolution. *Science* **2001**, 292, 883–96.
- (5) Frank, J.; Agrawal, R. A ratchet-like inter-subunit reorganization of the ribosome during translocation. *Nature* **2000**, 406, 318–322.
- (6) Valle, M.; Zavialov, A.; Sengupta, J.; Rawat, U.; Ehrenberg, M.; Frank, J. Locking and unlocking of ribosomal motions. *Cell* **2003**, *114*, 123–134.

- (7) Beckmann, R.; Spahn, C.; Eswar, N.; Helmers, J.; Penczek, P.; Sali, A.; Frank, J.; Blobel, G. Architecture of the protein-conducting channel associated with the translating 80S ribosome. *Cell* **2001**, *107*, 361–372.
- (8) Hassan, A.; Byju, S.; Freitas, F. C.; Roc, C.; Pender, N.; Nguyen, K.; Kimbrough, E. M.; Mattingly, J.; Gonzalez, R. L.; de Oliveira, R. J.; et al.Ratchet, Swivel, Tilt and Roll: A Complete Description of Subunit Rotation in the Ribosome. *bioRxiv*2022, DOI: 10.1101/2022.06.22.497108.
- (9) Rodnina, M. V.; Savelsbergh, A.; Wintermeyer, W. Dynamics of translation on the ribosome: molecular mechanics of translocation. *FEMS Microbiol Rev.* **1999**, 23, 317–33.
- (10) Johansson, M.; Bouakaz, E.; Lovmar, M.; Ehrenberg, M. The kinetics of ribosomal peptidyl transfer revisited. *Mol. Cell* **2008**, *30*, 589–98
- (11) Johansson, M.; Bouakaz, E.; Lovmar, M.; Ehrenberg, M. The kinetics of ribosomal peptidyl transfer revisited. *Molecular cell* **2008**, 30, 589–598.
- (12) Rodnina, M. V.; Wintermeyer, W. The ribosome as a molecular machine: the mechanism of tRNA-mRNA movement in translocation. *Biochem. Soc. Trans.* **2011**, *39*, 658–62.
- (13) Blanchard, S. C.; Gonzalez, R. L.; Kim, H. D.; Chu, S.; Puglisi, J. D. tRNA selection and kinetic proofreading in translation. *Nat. Struct Mol. Biol.* **2004**, *11*, 1008–14.
- (14) Lee, T.-H.; Blanchard, S. C.; Kim, H. D.; Puglisi, J. D.; Chu, S. The role of fluctuations in tRNA selection by the ribosome. *Proc. Natl. Acad. Sci. U. S. A.* **2007**, *104*, 13661–13665.
- (15) Kim, H. D.; Puglisi, J. D.; Chu, S. Fluctuations of transfer RNAs between classical and hybrid states. *Biophys. J.* **2007**, 93, 3575–3582.
- (16) Cornish, P. V.; Ermolenko, D. N.; Noller, H. F.; Ha, T. Spontaneous intersubunit rotation in single ribosomes. *Mol. Cell* **2008**, *30*, 578–88.
- (17) Fei, J.; Kosuri, P.; MacDougall, D. D.; Gonzalez, R. L. Coupling of Ribosomal L1 Stalk and tRNA Dynamics during Translation Elongation. *Mol. Cell* **2008**, *30*, 348–359.
- (18) Fei, J.; Bronson, J. E.; Hofman, J. M.; Srinivas, R. L.; Wiggins, C. H.; Gonzalez, R. L. Allosteric collaboration between elongation factor G and the ribosomal L1 stalk directs tRNA movements during translation. *Proc. Natl. Acad. Sci. U. S. A.* **2009**, *106*, 15702–7.
- (19) Cornish, P.; Ermolenko, D.; Staple, D.; Hoang, L.; Hickerson, R.; Noller, H.; Ha, T. Following movement of the L1 stalk between three functional states in single ribosomes. *Proc. Natl. Acad. Sci. U.S.A.* **2009**, *106*, 2571–2576.
- (20) Chen, C.; Stevens, B.; Kaur, J.; Cabral, D.; Liu, H.; Wang, Y.; Zhang, H.; Rosenblum, G.; Smilansky, Z.; Goldman, Y. E.; et al. Single-molecule fluorescence measurements of ribosomal translocation dynamics. *Mol. Cell* **2011**, *42*, 367–77.
- (21) Salsi, E.; Farah, E.; Dann, J.; Ermolenko, D. N. Following movement of domain IV of elongation factor G during ribosomal translocation. *Proc. Natl. Acad. Sci. U.S.A.* **2014**, *111*, 15060–15065.
- (22) Ratje, A.; Loerke, J.; Mikolajka, A.; Brünner, M.; Hildebrand, P. W.; Starosta, A.; Dönhöfer, A.; Connell, S.; Fucini, P.; Mielke, T.; et al. Head swivel on the ribosome facilitates translocation by means of intra-subunit tRNA hybrid sites. *Nature* **2010**, *468*, 713–716.
- (23) Nguyen, K.; Whitford, P. C. Steric interactions lead to collective tilting motion in the ribosome during mRNA-tRNA translocation. *Nat. Commun.* **2016**, *7*, 10586–10586.
- (24) Kurkcuoglu, O.; Doruker, P.; Sen, T.; Kloczkowski, A.; Jernigan, R. L. The ribosome structure controls and directs mRNA entry, translocation and exit dynamics. *Phys. Biol.* **2008**, *5*, 046005.
- (25) Ramrath, D. J. F.; Yamamoto, H.; Rother, K.; Wittek, D.; Pech, M.; Mielke, T.; Loerke, J.; Scheerer, P.; Ivanov, P.; Teraoka, Y.; et al. The complex of tmRNA–SmpB and EF-G on translocating ribosomes. *Nature* **2012**, *485*, 526–529.
- (26) Guyomar, C.; D'Urso, G.; Chat, S.; Giudice, E.; Gillet, R. Structures of tmRNA and SmpB as they transit through the ribosome. *Nat. Commun.* **2021**, *12*, 4909.
- (27) Noel, J. K.; Levi, M.; Raghunathan, M.; Lammert, H.; Hayes, R. L.; Onuchic, J. N.; Whitford, P. C. SMOG 2: A Versatile Software

- Package for Generating Structure-Based Models. *PLoS Comput. Biol.* **2016**, 12, No. e1004794.
- (28) Wasserman, M. R.; Alejo, J. L.; Altman, R. B.; Blanchard, S. C. Multiperspective smFRET reveals rate-determining late intermediates of ribosomal translocation. *Nat. Struct. Mol. Biol.* **2016**, *23*, 333–41.
- (29) Onuchic, J.; Socci, N.; Luthey-Schulten, Z.; Wolynes, P. Protein folding funnels: The nature of the transition state ensemble. *Fold Des* **1996**, *1*, 441–450.
- (30) Das, P.; Moll, M.; Stamati, H.; Kavraki, L.; Clementi, C. Low-dimensional, free-energy landscapes of protein-folding reactions by nonlinear dimensionality reduction. *Proc. Natl. Acad. Sci. U.S.A.* **2006**, 103, 9885–9890.
- (31) Best, R. B.; Hummer, G. Coordinate-dependent diffusion in protein folding. *Proc. Natl. Acad. Sci. U. S. A.* **2010**, *107*, 1088–1093.
- (32) Zhang, Z.; Chan, H. S. Transition paths, diffusive processes, and preequilibria of protein folding. *Proc. Natl. Acad. Sci. U.S.A.* **2012**, 109, 20919–20924.
- (33) Cho, S. S.; Levy, Y.; Wolynes, P. G. P versus Q: structural reaction coordinates capture protein folding on smooth landscapes. *Proc. Natl. Acad. Sci. U.S.A.* **2006**, *103*, 586–91.
- (34) Best, R. B.; Hummer, G. Reaction coordinates and rates from transition paths. *Proc. Natl. Acad. Sci. U.S.A.* **2005**, *102*, 6732–6737.
- (35) Best, R. B.; Hummer, G.; Eaton, W. A. Native contacts determine protein folding mechanisms in atomistic simulations. *Proc. Natl. Acad. Sci. U.S.A.* **2013**, *110*, 17874–17879.
- (36) Chan, H. S.; Zhang, Z.; Wallin, S.; Liu, Z. Cooperativity, Local-Nonlocal Coupling, and Nonnative Interactions: Principles of Protein Folding from Coarse-Grained Models. *Annu. Rev. Phys. Chem.* **2011**, 62, 301–326.
- (37) Hyeon, C.; Thirumalai, D. Can energy landscape roughness of proteins and RNA be measured by using mechanical unfolding experiments? *Proc. Natl. Acad. Sci. U. S. A.* **2003**, *100*, 10249–53.
- (38) Best, R.; Paci, E.; Hummer, G.; Dudko, O. Pulling direction as a reaction coordinate for the mechanical unfolding of single molecules. *J. Phys. Chem. B* **2008**, *112*, 5968–5976.
- (39) Hyeon, C.; Morrison, G.; Pincus, D. L.; Thirumalai, D. Refolding dynamics of stretched biopolymers upon force quench. *Proc. Natl. Acad. Sci. U.S.A.* **2009**, *106*, 20288–93.
- (40) Hummer, G. Position-dependent diffusion coefficients and free energies from Bayesian analysis of equilibrium and replica molecular dynamics simulations. *New J. Phys.* **2005**, *7*, 34–34.
- (41) Krivov, S. V. On reaction coordinate optimality. J. Chem. Theory Comput. 2013, 9, 135–146.
- (42) Rohrdanz, M. A.; Zheng, W.; Maggioni, M.; Clementi, C. Determination of reaction coordinates via locally scaled diffusion map. *Chem. Phys.* **2011**, *134*, 124116.
- (43) Pérez-Hernández, G.; Paul, F.; Giorgino, T.; De Fabritiis, G.; Noé, F. Identification of slow molecular order parameters for Markov model construction. *J. Chem. Phys.* **2013**, *139*, 015102.
- (44) Noé, F.; Banisch, R.; Clementi, C. Commute Maps: Separating Slowly Mixing Molecular Configurations for Kinetic Modeling. *J. Chem. Theory Comput.* **2016**, *12*, 5620–5630.
- (45) Noel, J. K.; Chahine, J.; Leite, V. B. P.; Whitford, P. C. Capturing Transition Paths and Transition States for Conformational Rearrangements in the Ribosome. *Biophys. J.* **2014**, *107*, 2881.
- (46) Levi, M.; Whitford, P. C. Dissecting the energetics of subunit rotation in the ribosome. *J. Phys. Chem. B* **2019**, 123, 2812–2923.
- (47) Bock, L. V.; Blau, C.; Schröder, G. F.; Davydov, I. I.; Fischer, N.; Stark, H.; Rodnina, M. V.; Vaiana, A. C.; Grubmüller, H. Energy barriers and driving forces in tRNA translocation through the ribosome. *Nat. Struct. Mol. Biol.* **2013**, *20*, 1390–1396.
- (48) Levi, M.; Nguyen, K.; Dukaye, L.; Whitford, P. C. Quantifying the Relationship between Single-Molecule Probes and Subunit Rotation in the Ribosome. *Biophys. J.* **2017**, *113*, 2777–2786.
- (49) Whitford, P. C.; Noel, J. K.; Gosavi, S.; Schug, A.; Sanbonmatsu, K. Y.; Onuchic, J. N. An all-atom structure-based potential for proteins: bridging minimal models with all-atom empirical forcefields. *Prot. Struct. Funct. Bioinfo.* 2009, 75, 430–441.

- (50) Oliveira, A. B.; Contessoto, V. G.; Hassan, A.; Byju, S.; Wang, A.; Wang, Y.; Dodero-Rojas, E.; Mohanty, U.; Noel, J. K.; Onuchic, J. N.; Whitford, P. C.; et al. SMOG 2 and OpenSMOG: Extending the limits of structure-based models. *Protein Sci.* 2022, 31, 158–172.
- (51) Jenner, L. B.; Demeshkina, N.; Yusupova, G.; Yusupov, M. Structural aspects of messenger RNA reading frame maintenance by the ribosome. *Nat. Struct. Mol. Biol.* **2010**, *17*, 555.
- (52) Van Der Spoel, D.; Lindahl, E.; Hess, B.; Groenhof, G.; Mark, A. E.; Berendsen, H. J. GROMACS: fast, flexible, and free. *J. Comput. Chem.* **2005**, *26*, 1701–1718.
- (53) Lindahl, E.; Hess, B.; van der Spoel, D. GROMACS 3.0: A package for molecular simulation and trajectory analysis. *J. Mol. Mod.* **2001**, *7*, 306–317.
- (54) Hess, B.; Kutzner, C.; van der Spoel, D.; Lindahl, E. GROMACS 4: Algorithms for highly efficient, load-balanced, and scalable molecular simulation. *J. Chem. Theory Comput.* **2008**, *4*, 435–447.
- (55) Abraham, M. J.; Murtola, T.; Schulz, R.; Páll, S.; Smith, J. C.; Hess, B.; Lindahl, E. GROMACS: High performance molecular simulations through multi-level parallelism from laptops to supercomputers. *SoftwareX* **2015**, *1*–2, 19–25.
- (56) Tobias, D.; Martyna, G.; Klein, M. Molecular-dynamics simulations of a protein in the canonical ensemble. *J. Phys. Chem-Us* **1993**, *97*, 12959–12966.
- (57) Whitford, P. C.; Geggier, P.; Altman, R. B.; Blanchard, S. C.; Onuchic, J. N.; Sanbonmatsu, K. Y. Accommodation of aminoacyltRNA into the ribosome involves reversible excursions along multiple pathways. *RNA* **2010**, *16*, 1196–1204.
- (58) Yang, H.; Bandarkar, P.; Horne, R.; Leite, V. B.; Chahine, J.; Whitford, P. C. Diffusion of tRNA inside the ribosome is position-dependent. *J. Chem. Phys.* **2019**, *151*, 085102.
- (59) Duncan, T. E. On the calculation of mutual information. SIAP 1970, 19, 215–220.
- (60) Cover, T. M. Elements of Information Theory; John Wiley & Sons, NJ, 1999.
- (61) Desai, B. J.; Gonzalez, R. L. Multiplexed genomic encoding of non-canonical amino acids for labeling large complexes. *Nat. Chem. Biol.* **2020**, *16*, 1129–1135.
- (62) Dunkle, J. A.; Wang, L.; Feldman, M. B.; Pulk, A.; Chen, V. B.; Kapral, G. J.; Noeske, J.; Richardson, J. S.; Blanchard, S. C.; Cate, J. H. D. Structures of the Bacterial Ribosome in Classical and Hybrid States of tRNA Binding. *Science* **2011**, 332, 981–984.
- (63) Schuwirth, B. S.; Borovinskaya, M. A.; Hau, C. W.; Zhang, W.; Vila-Sanjurjo, A.; Holton, J. M.; Cate, J. H. D. Structures of the Bacterial Ribosome at 3.5 Å Resolution. *Science* **2005**, *310*, 827–834.
- (64) Carbone, C. E.; Loveland, A. B.; Gamper, H. B.; Hou, Y.-M.; Demo, G.; Korostelev, A. A. Time-resolved cryo-EM visualizes ribosomal translocation with EF-G and GTP. *Nat. Commun.* **2021**, *12*, 124116.
- (65) Akbar, S.; Bhakta, S.; Sengupta, J. Structural insights into the interplay of protein biogenesis factors with the 70S ribosome. *Structure* **2021**, *29*, 755–767.
- (66) Zhou, J.; Lancaster, L.; Donohue, J. P.; Noller, H. F. Crystal Structures of EF-G-Ribosome Complexes Trapped in Intermediate States of Translocation. *Science* **2013**, *340*, 1236086.
- (67) Dimura, M.; Peulen, T. O.; Hanke, C. A.; Prakash, A.; Gohlke, H.; Seidel, C. A. Quantitative FRET studies and integrative modeling unravel the structure and dynamics of biomolecular systems. *Curr. Opin. Struct. Biol.* **2016**, *40*, 163–185.
- (68) Dimura, M.; Peulen, T.-O.; Sanabria, H.; Rodnin, D.; Hemmen, K.; Hanke, C. A.; Seidel, C. A.; Gohlke, H. Automated and optimally FRET-assisted structural modeling. *Nat. Commun.* **2020**, *11*, 5394.
- (69) Song, J.; Gomes, G.-N.; Shi, T.; Gradinaru, C. C.; Chan, H. S. Conformational heterogeneity and FRET data interpretation for dimensions of unfolded proteins. *Biophysical journal* **2017**, *113*, 1012–1024.
- (70) Wang, A.; Levi, M.; Mohanty, U.; Whitford, P. C. Diffuse ions coordinate dynamics in a ribonucleoprotein assembly. *J. Am. Chem. Soc.* **2022**, *144*, 9510–9522.

- (71) Baibakov, M.; Patra, S.; Claude, J. B.; Moreau, A.; Lumeau, J.; Wenger, J. Extending Single-Molecule Förster Resonance Energy Transfer (FRET) Range beyond 10 Nanometers in Zero-Mode Waveguides. ACS Nano 2019, 13, 8469–8480.
- (72) Uemura, S.; Aitken, C. E.; Korlach, J.; Flusberg, B. A.; Turner, S. W.; Puglisi, J. D. Real-time tRNA transit on single translating ribosomes at codon resolution. *Nature* **2010**, *464*, 1012–1017.
- (73) Chen, J.; Coakley, A.; O'Connor, M.; Petrov, A.; O'Leary, S. E.; Atkins, J. F.; Puglisi, J. D. Coupling of mRNA Structure Rearrangement to Ribosome Movement during Bypassing of Non-coding Regions. *Cell* **2015**, *163*, 1267–1280.
- (74) Humphrey, W.; Dalke, A.; Schulten, K. VMD: Visual molecular dynamics. *J. Mol. Graph.* **1996**, *14*, 33–38.
- (75) Tourigny, D. S.; Fernández, I. S.; Kelley, A. C.; Ramakrishnan, V. Elongation Factor G Bound to the Ribosome in an Intermediate State of Translocation. *Science* **2013**, *340*, 1235490.

□ Recommended by ACS

Protein Dynamics and Enzymatic Catalysis

Steven D. Schwartz.

MARCH 21, 2023

THE JOURNAL OF PHYSICAL CHEMISTRY B

READ 🗹

Challenges in Inferring the Directionality of Active Molecular Processes from Single-Molecule Fluorescence Resonance Energy Transfer Trajectories

Aljaž Godec and Dmitrii E. Makarov

DECEMBER 25, 2022

THE JOURNAL OF PHYSICAL CHEMISTRY LETTERS

READ 🗹

The Effect of Time Resolution on Apparent Transition Path Times Observed in Single-Molecule Studies of Biomolecules

Dmitrii E. Makarov, Eli Pollak, et al.

OCTOBER 04, 2022

THE JOURNAL OF PHYSICAL CHEMISTRY B

READ 🗹

Impact of the Cellular Environment on Adenosine Triphosphate Conformations

Meredith M. Rickard, Taras V. Pogorelov, et al.

OCTOBER 13, 2022

THE JOURNAL OF PHYSICAL CHEMISTRY LETTERS

READ **C**

Get More Suggestions >